HUMAN LOWER LIMB MOTION PATTERN RECOGNITION BASED ON MULTI-SENSOR FUSION
/
基于多传感器融合的人体下肢运动模式识别

Cuihong LIU[1)], Yanbo HAN[2)], Xiangwen SONG[2)], Shipeng ZHANG[1)], Na HAN[2)], Meng ZOU[2)], Liyan WU[*1)]
[1)]College of Engineering, Shenyang Agricultural University, Shenyang, China;
[2)]Key Lab for Bionics Engineering of Education Ministry, Jilin University, Changchun, China
[*)]*Corresponding author: Tel: 15942098712; E-mail: wly78528@syau.edu.cn*
DOI: https://doi.org/10.35633/inmateh-75-78

Keywords: *Human lower limb; Gait Mode Recognition; Plantar Pressure Measurement System; Inertial Measurement Units; Intelligent Prostheses*

ABSTRACT

One of the essentials of intelligent prosthetics design is to recognize the wearer's movement intention, to provide the wearer with the corresponding control strategy and movement assistance. The 11 independent gait patterns and 5 transformed gait patterns are recognized by the self-designed human lower limb motion data measurement system. The human gait pattern is classified by the linear discriminant analysis (LDA) classifier, and the recognition accuracy is evaluated by K-fold Cross Validation(K-CV). The average recognition accuracy of independent gait patterns is 90.91%. In the independent gait pattern, the lowest recognition accuracy of DS1 gait phase is 90.53%, and the highest recognition accuracy of SS2 gait phase is 91.36%. The overall average recognition accuracy of the transformed gait pattern is 92.67%, the lowest recognition accuracy of DS1 gait phase is 91.93%, and the highest recognition accuracy of SS1 gait phase is 93.31%. The main reason affecting the recognition accuracy is that some gait patterns have similar motion characteristics. The method proposed in this study can accurately predict the wearer's locomotion mode and serves as a reference for gait pattern recognition, prediction, and control strategies in intelligent prosthetic devices.

摘要

智能假肢设计的关键之一是识别佩戴者的运动意图，为佩戴者提供相应的控制策略和运动辅助。通过自主设计的人体下肢运动数据测量系统对11 种独立步态模式和5 种变换步态模式进行识别。采用线性判别分析（LDA）分类器对人体步态模式进行分类，并采用 K-fold 交叉验证（K-CV）对识别精度进行评价。独立步态模式的平均识别准确率为90.91%。在独立步态模式下，DS1 步态相位的识别准确率最低为90.53%，SS2 步态相位的识别准确率最高为 91.36%。变换步态模式的整体平均识别准确率为 92.67%，DS1 步态相位的最低识别准确率为 91.93%，SS1 步态相位的最高识别准确率为 93.31%。影响识别精度的主要原因是某些步态模式具有相似的运动特征。本文提出的方法可以准确预测佩戴者的运动模式，为智能假肢的步态模式识别、预测和控制策略提供参考。

INTRODUCTION

Lower limb amputation affects daily life. Although passive prostheses can meet the basic daily use of amputees, the wearer presents asymmetrical gait patterns in performing daily activities *(Zhu et al., 2014; Windrich et al., 2016; Dey et al., 2020)*. To compare with the able-bodied individuals, the amputees need to consume 20-30% extra metabolic energy in movement *(Au et al., 2009)*. Intelligent prostheses, as a medical device that can simulate the human-machine relationship between amputee and prosthesis to the maximum extent, are attracting more and more attention *(Tucker et al., 2015; Silva Júnior et al., 2015; Yang et al., 2016; Hernandez and Yu, 2022; Yue et al., 2023).*

The study of locomotion mode is one of the important contents of intelligent prostheses. By collecting and analyzing relevant signals, the basic information of human movement can be extracted, and then different control strategies can be selected by judging the movement to ensure the smooth and labor-saving of the wearer. At present, the signals used for the study of locomotion mode are mainly divided into mechanical signals (such as gyroscopes, accelerometers, goniometers and magnetometers) *(Bisio et al., 2016; Quintero et al., 2016)* and bioelectric signals (electromyography (EMG) is a widely used bioelectric signal) *(Bakina et al., 2018; Chen et al., 2015; Wang et al., 2016).*

Cuihong Liu, Prof. Ph.D. Eng.; Yanbo Han, Xiangwen Song, Shipeng Zhang, Na han, M.S. Stud. Eng.; Meng Zou and Liyan Wu, Prof. Ph.D. Eng.

Nazarpour et al. recognized the locomotion mode based on EMG signals, utilized higher order statistics of EMG signal to classify four primitive motions, i.e., elbow flexion, elbow extension, forearm supination, and forearm pronation. The results indicated that the proposed approach provided higher identification rates *(Nazarpour et al., 2007)*. Liu et al. collected the EMG signals of two able-bodied subjects and two unilateral transfemoral amputees during normal walking, compared and evaluated three kinds of adaptive classifiers off-line *(Liu et al., 2017)*. The entropy-based adaptation was implemented for real-time human-in-the-loop prosthesis control. The online evaluation showed that the developed novel adaptive strategy may further enhance the reliability of neurally controlled prosthetic legs. Wang et al. proposed a wearable plantar pressure measurement system, which identified five locomotion modes through four force sensors mounted on insoles, and the average recognition errors of four phases of the five patterns were 19.6%, 12.6%, 5.2%, and 6.3% respectively *(Wang et al., 2012)*. Young et al. used mechanical sensors to identify five motion modes of walking on level ground, ramp and stairs, with an overall accuracy of 93.9% *(Young et al., 2013)*. Meng et al. collected EMG signals and linear acceleration of 10 able-bodied subjects in seven locomotion activities, such as sitting, standing and walking horizontally. By comparing four classifiers, the results show that the SVM model with a sliding window size of 80ms has the best recognition performance. EMG signal fusion not only improves the recognition accuracy of steady-state motion from 90% (only using acceleration data) to 98% (using data fusion), but also can predict the next steady-state motion *(Meng et al., 2021)*.

EMG signal will change with the change of electrode conductivity, electrophysiology, space, user and other factors, and the myoelectric decoding algorithms is very demanding *(Sensinger et al., 2009; Jain et al., 2012; Young and Ferris, 2016; Fan et al., 2024)*. Compared with bioelectric signals, mechanical signals are more mature, smaller in size and highly integrated *(Ambrozic et al., 2014; Gorsic et al., 2014; Yuan et al., 2017)*. The acquisition of mechanical signals is mainly through accelerometers, gyroscopes, pressure sensors and other devices *(Adapala et al., 2013; Parri et al., 2017; Hussain et al., 2019)*. For example, Hartmann et al. proposed an online human activity recognition (HAR) system, in which wearable sensors (such as inertial measurement units) acquire data and identify activities through hidden Markov models *(Hartmann et al., 2022)*. On the other hand, data provided by multiple sensors is superior to data provided by a single sensor in theory *(Khaleghi et al., 2013)*. Multi-sensing technology can reduce the power consumption while achieving more abundant functions, because of the development of microcomputer system and electronic technology. Hartmann et al. proposed a multi-sensor data collector (CSL-SHARE) for HAR. sensors used include triaxial accelerometers, triaxial gyroscopes, sEMG sensors, biaxial electrogoniometer, and airborne microphone. The accuracy of the CSL-SHARE dataset reached 96.1% *(Liu et al., 2021; Hartmann et al., 2022)*. Smart knee bandage is a new method, sensors are fixed inside knee bandages and socks, and evaluates the movement posture of patients through IMU and pressure sensors, so as to obtain the movement and rehabilitation of patients *(Haladjian et al., 2017; Haladjian et al., 2018)*. It is worth noting that Hartmann et al. defined six High-Level Features of the subjects, obtained the information base by deploying different sensor carriers, and learned the relationship between the characteristic values of each activity and the sensor data through classification algorithms, so as to carry out pattern recognition. This method is a relatively advanced research content, and the recognition accuracy rate based on the CSL-SHARE and UniMiB SHAR datasets reaches 89.7% and 67.3%, respectively *(Hartmann et al., 2023)*. In conclusion, the study of locomotion mode based on multi-sensor fusion has received more attention and development *(Varol et al., 2010; Huang et al., 2011; Luo et al., 2023)*. Linear Discriminant analysis（LDA）, also known as Fisher Linera Discriminant (FLD), is a classic algorithm for pattern recognition. It was introduced into the field of pattern recognition and artificial intelligence by Belhumeur in 1996. It is an effective feature extraction method. By this, the interclass dispersion matrix of projected pattern samples can be maximized, while the intra-class dispersion matrix is minimized *(Tharwat et al., 2017)*. This method has been successfully applied to HAR. Hartmann et al. also compared the differences between the methods. The research showed that the poor recognition performance when it was used in a single read, but its transformation helped to improve the overall recognition performance, which was conducive to identifying most activities *(Hartmann et al., 2021)*, and the evaluation performance of LDA based on HMM could be improved by 4 percentage *(Hartmann et al., 2020)*. Therefore, the LDA method is adopted in this paper.

This study aims to accurately recognize human lower limb locomotion mode through the method of multi-sensor fusion. First a human lower limb motion data measurement system was developed. The measurement system consists of two inertial measurement units (IMUs) and a plantar pressure measurement system (PPS, containing three force sensors for each foot). The kinematic and dynamic parameters of the human motion are measured by IMU and PPS, respectively.

Linear discriminant analysis (LDA) was used to identify 11 independent gaits and 5 transformed gaits. Gait recognition helps to provide the right control strategy for the intelligent prosthesis, thus activating the corresponding drive mode to assist the amputee's movement. On the basis of ensuring the recognition accuracy, the number of motion patterns increased in this study. Outcomes covers the daily use of subjects, providing a reference for HAD and intelligent wearable devices.

MATERIALS AND METHODS

Human lower limb motion data measurement system

The key to accurately recognize locomotion mode is the reliability and stability of measurement system. The human lower limb motion data measurement system is presented, and its reliability and environmental adaptability is also verified.

The daily movement of human lower limbs includes the kinematic information of legs and the dynamic information between the sole and the ground. Only by collecting this information comprehensively, can the motion state of lower limbs be accurately described. The spatial motion information of human lower limbs is complicated, and it is difficult to cover the daily activity posture with a single sensor. Therefore, the composition of motion data measurement system designed in this paper needs two sensors, inertial measurement unit (IMU) and plantar-pressure measurement unit, which can make up for each other's shortcomings and facilitate us to analyze human lower limb gait more comprehensively. Secondly, due to the complexity of human movement, the data collected by the same type of single sensor can't completely reflect the information contained in the movement to a certain extent. To sum up, the composition of the human lower limb motion data measurement system is shown in Fig. 1. The system consists of two inertial measurement units (IMUs), six thin-film force sensors, an Analog to digital conversion module (A/D Mod) and a computer. The information detected by IMUs and plantar pressure sensors enables comprehensive analysis and recognition of lower limb gaits.

The IMU is an MTi-30 AHRS (Attitude and Heading Reference System) produced by Xsens of the Netherlands (fig. 1b). Motion capture of human lower limbs can be realized by IMU sensor. However, it is difficult for a single IMU sensor to accurately judge the movement with the gait cycle. Two IMU sensors are selected and fixed on the thigh and shank, which can reflect the complete information of the movement. The MT Manager software is used to display in real-time the three-dimensional motion information of the human lower limbs collected by the IMU, and it can also store the experimental data.

In this paper, the force sensor, FlexiForce A401, is a thin film sensor (fig. 1d), which is produced by Tek scan of America. This sensor integrates the measurement signal and processing circuit and obtains drift-free signal data through its built-in low-power processor.

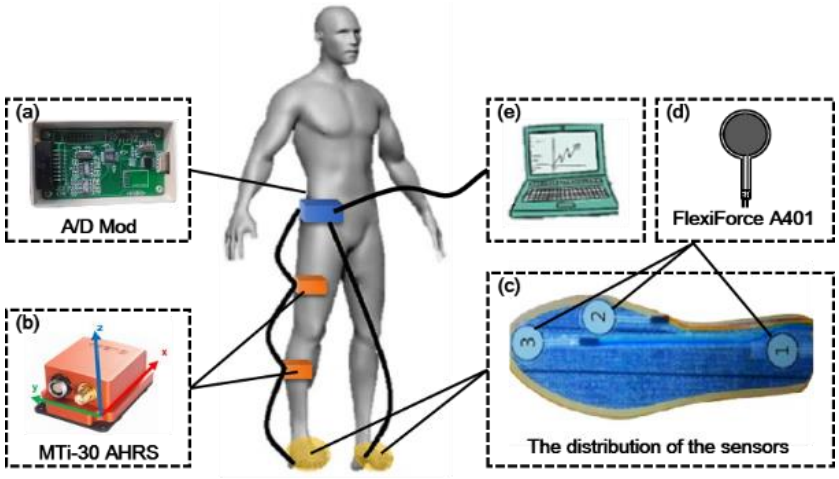

Fig. 1 - Human lower limb motion data measurement system

A single sensor cannot completely measure the pressure change of the entire plantar during the movement, and if the pressure sensing area is small or the location is inappropriate, it will inevitably cause the loss of the plantar pressure information. In this paper, the pressure test system (fig. 2a) is used to test the plantar pressure. In the experiment, three healthy volunteers walked through the plantar pressure test bench with bare feet. After collecting the data of the changes of plantar pressure, the plantar region was partitioned and the stress situation of each region was analyzed. The placement position of the plantar region sensor was determined by observing several zones with the largest strain (fig. 2b).

Fig. 2 - Position of the plantar region sensor

(a) Pressure test system; (b) Volunteer plantar pressure

Three sensors are attached to each insole to form a plantar pressure measurement system (PPS), the distribution of the sensors is shown in Figure 1c, the calcaneus tuberosity (sensor 1), the first metatarsal bone (sensor 2) and the hallux toe (sensor 3).

A/D Mod is installed on the waist of the wearer to process and convert the signals output by the sensor. To reduce the delay of data transmission, the transmission cable is used, and the computer is connected by USB to realize the transmission and storage of sensor data, and the analysis and visualization of IMU and force sensor data are realized.

Plantar pressure system calibration

IMU realizes data conversion through its built-in low-power processor. But the force sensor (FlexiForce A401) is a tiny thin force-sensitive resistor which varies with the vertical pressure. To ensure the accuracy of the value, it is necessary to carry out calibration.

Weight of 1-10 kg is used in the calibration. The weight is increased in increments of 1 kg and the corresponding force is 9.8 N. In the test, to ensure full contact between the weight and the force sensor, the weight is placed vertically, while the applied pressure value and the output value are recorded. The linear fitting was carried out by Matlab and the resulting calibration equation is shown in Equation 1:

$$V_{out} = 0.0028 \times F + 1.1128 \quad (1)$$

where V_{out} is the output value of the force sensor, F is the applied pressure. The residual norm of linear fitting is 0.0101, and the residual norm is < 0.05. The results show that there is a good linear relationship between the output value and the applied pressure value (fig. 3). In order to identify various gaits more intuitively, the calibration equation was used to convert the voltage output of the sensors into the pressure value, and then the test results were analyzed.

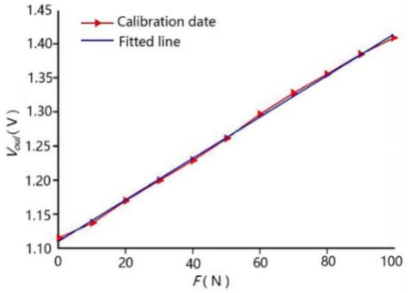

Fig. 3 - The fitting details

Adaptability to different ground surfaces

The contact force that is obtained by the plantar pressure measurement system may be affected by the type of surface. To ensure the output stability of different surfaces, the adaptability of 6 mm rubber floor, 3 mm carpet floor and 9 mm wood floor is carried out. The experiment process is described in Fig. 4.

Fig. 4 - The experiment process

(a) Rubber floor; (b) Carpet floor; (c) Wood floor

The experiment is carried out by an able-bodied subject, 25 years old, male, with weight of 75 kg and height of 1.72 m. The subject is asked to walk at a normal, comfortable pace across three different surfaces under laboratory conditions. The subject walks for 3 complete gait cycles each time, and the pressure between the foot and the ground is collected during the walking. The pressure data are shown in Fig. 5.

Fig. 5 shows the data collected by three force sensors of a plantar pressure measurement system, and data of different ground types are represented by curves of different colors. The maximum signal difference of each force sensor in three different ground types is 6.6%, 4.5% and 7.9%, respectively. And the maximum signal difference is always around the peak of the signal. These results indicate that the signals of three force sensors in different areas of the same foot have similarities on different ground. In other words, the plantar pressure measurement system adapts to different surfaces.

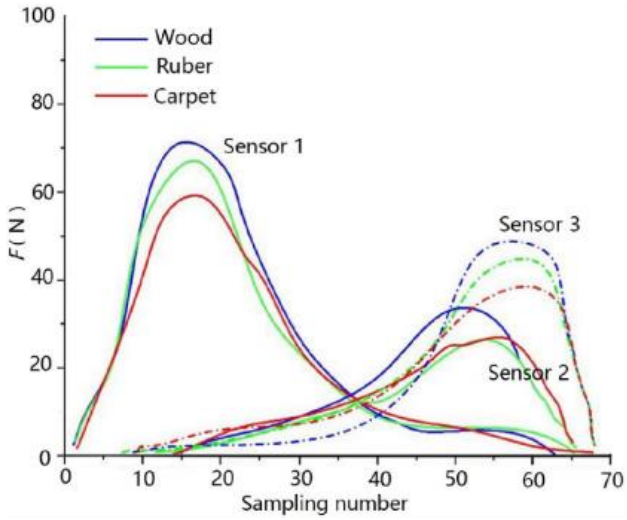

Fig. 5 - The pressure data on three surface types

The process of experiment

In our study, 10 able-bodied subjects are recruited. Their average age is 24.7 ± 1.4 years, average weight is 69.4 ± 10.7 kg, average height is 1.773 ± 0.054 m, and average foot size is 26.1 ± 0.5 cm. The positions of the sensors are shown in Fig. 1 10 able-bodied subjects are given adaptive exercises after wearing the device.

In this paper, 11 independent gait patterns and 5 transformed gait patterns are designed to study the locomotion mode. The number of experiment groups in each gait pattern is 15. The type of gait pattern and gait cycles are shown in Table 1.

Table 1

The number of trials for each pattern and gait cycles for each trial

Type	Gait patterns	Trial number	Gait cycles
Independent gait patterns	Sitting (SI)	15	–
	Standing (ST)	15	–
	Level-Walking (LW)	15	5
	Level-Fast Walking (LFW)	15	5
	Soil Walking (SW)	15	5
	Stair Ascending (SA)	15	2
	Stair Descending (SD)	15	2
	Ramp Ascending (RA)	15	2
	Ramp Descending (RD)	15	2
	Soil Ramp Ascending (SRA)	15	2
	Soil Ramp Descending (SRD)	15	2
Transformed gait patterns	Level-Walking - Ramp Ascending (LW - RA)	15	4
	Level-Walking - Stair Ascending (LW - SA)	15	4
	Level-Walking - Stair Descending (LW - SD)	15	4
	Soil Walking - Soil Ramp Ascending (SW - SRA)	15	4
	Standing - Sitting (ST-SI)	15	–

The requirements of the test of independent gait are as follows. For the pattern of SI, the subjects are asked to sit on a 42 cm high chair in a normal, comfortable position (Fig. 6a). For the ST test, the subjects are asked to stand still on the ground, and the subjects are relatively relaxed, and maintain a steady body (Fig. 6b). The LW and LFW require subjects to walk 5 steps on a straight hard surface, the speed is scheduled walking speed and slightly higher than daily walking speed respectively (Fig. 6c). The walking conditions of SW are the same as LW.

The difference is that the road surface of SW is soft soil, and the soil needs to be turned over before and after walking (Fig. 6d). The test environment of SA and SD is four steps, the width of the step is 0.4 m, and the height is 0.15 m. The subjects need to walk at a comfortable pace and posture (Fig. 6e). RA and RD are tested on the hard floor on the ramp, and the slope on the hard floor slope is 5 m in length, 1 m in width and 18.5° in inclination angle. To maintain normal walking speed and posture (Fig. 6f). The difference between SRA and SRD and RA and RD is that the road surface of SRA and SRD is soft soil, the soil needs to be turned over before and after walking to ensure the soft soil (Fig. 6g).

Fig. 6 - Test of independent and transformed gait pattern

(a) SI; (b) ST; (c) LW and LFW; (d) SW; (e) SA and SD; (f) RA and RD; (g) SRA and SRD; (h) LW-RA; (i) SW-SRA

The requirements of the test of transformed gait are as follows. The walking conditions of LW-RA mode (Fig. 6h), LW-SA mode, LW-SD mode and SW-SRA mode (Fig. 6i) are consistent. The subjects are advised to walk 2 steps on each road. The difference between them is that the two types of pavements are different from each other. See independent gait for a detailed description. In ST-SI, the subjects stand up at first and then sit on a chair in a way that is normal for them.

During the experiment, 10 subjects perform only one gait pattern each time, and each gait pattern is done in 15 groups. After each group of experiments, subjects are given a certain rest time. This method eliminates the impact of muscle fatigue on the data.

Data filtering processing

The Matlab software is employed, and statistical analysis methods are utilized for data processing. Moreover, algorithms such as time-domain analysis and principal component analysis are applied for eigenvalue extraction and other processing.

One of the keys of preprocessing is to remove the noise in the acquisition and transmission stages from the data. The data information necessary for the test can be obtained by data filtering. The data information comes from IMU and force sensor. In this paper, the IMU has a built-in classical Kalman filtering algorithm to filter the signals in real time. Kalman filter is a common algorithm for sensor data processing in the navigation field. Based on the linear system state equation, the Kalman filter optimally estimates the current state of the system by updating the collected data and the previous state estimation data. Compared with other filtering algorithms, it can process data in the time domain. The filter algorithm can be directly used to process sensor data in the actual power assisted control, and the algorithm uses less storage space and is easy to implement in the system.

Take the ADC (Analog-to-Digital Converter) curve of the original pressure at the position of the first metatarsal bone (Fig. 1c-sensor2) from RD gait pattern as an example (Fig. 7). The subjects start walking downhill from a stationary state, the initial pressure value was about 28 N, and began to decline with the right foot gradually raised. With the heel landing again, the pressure tended to peak again, and then the value changed periodically.

There is noise impact in the data of Fig. 7 The noise source mainly has 3 aspects: One is the body shake, then because of the signal conversion process, the last one is the friction between the sole and the insole. To eliminate the periodic interference in the data and effectively suppress the high-frequency jitter, the ADC value of plantar pressure was filtered by Savitzky-Golay sliding filter in this paper.

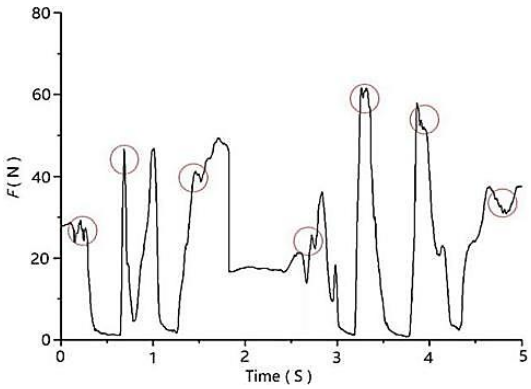

Fig. 7 - The value of the first metatarsal bone in RD gait patterns (before the filtering)

The core idea of Savitzky-Golay sliding filter is to fit the data in the window by the least squares method based on polynomials in the domain. Assume that the gait action data in a window of length p is x (i), i = -m, …, 0, …, m, same as 2m+1=p. In this window, K-order polynomials (Equation 2) are used to fit the original data.

$$f(i) = a_0 + a_1 i + a_2 i^2 + \cdots \ldots + a_k i^k = \sum_{n=0}^{k} a_n i^n \tag{2}$$

The residual of the least squares fitting ε is calculated through Equation 3.

$$\varepsilon = \sum_{i=-m}^{m} (f(i) - x(i))^2 = \sum_{i=-m}^{m} (\sum_{n=0}^{k} a_n i^n - x(i))^2 \tag{3}$$

To minimize the residual, the partial derivative of each polynomial coefficient needs to be 0, the derivative of it can be obtained through Equation 4.

$$\frac{\partial \varepsilon}{\partial a_r} = \sum_{i=-m}^{m} 2(f(i) - x(i)), i^r = 0 \tag{4}$$

where r =0, 1, ..., k-1, k.

The result after processing is shown in Equation 5.

$$\sum_{i=-m}^{m} (\sum_{n=0}^{k} a_n i^{n+r}) = \sum_{i=-m}^{m} x(i) i^r = \sum_{n=0}^{k} a_n (\sum_{i=-m}^{m} i^{n+r}) \tag{5}$$

where r =0, 1, ..., k-1, k, The linear system of equations on the fitting coefficients can be obtained by derivation, which can be expressed by the following matrix (Equation 6).

$$A^T A a = A^T X \tag{6}$$

where, $a = [a^0, a^1, \cdots, a^n]^T$, $X = [x(-m), \cdots, x(0), \cdots, x(m)]^T$,

The matrix A is defined as shown in Equation 7:

$$A = \begin{bmatrix} (-m)^k & (-m)^{k-1} & \cdots & (-m)^0 \\ \cdots & & & \cdots \\ \cdots & & & \cdots \\ m^k & m^{k-1} & \cdots & m^0 \end{bmatrix} \tag{7}$$

Finally, he result can be obtained as shown in Equation 8:

$$a = (A^T A)^{-1} A^T X \tag{8}$$

According to the coefficients, the results of k-order polynomial fitting to the original data can be obtained, and the filtering results can be obtained after discretization. After several tests, the best filtering effect with p =6 and k =1 is obtained. The ADC value of the first metatarsal bone in RD gait pattern after Savitzky-Golay filtering is shown in Fig. 8.

The gait segmentation

Gait Phase (GP) refers to the different states that a foot presents during a gait cycle. A gait cycle can be divided into several gait phases *(Wang and Hou, 2007)*. Gait phase is usually composed of two parts: Stance Phase and Swing Phase (Fig. 9). The phases of the gait cycle are relatively fixed during normal motion. It is believed that the stance phase takes up 60 – 65% of the time in a gait cycle *(Anwary et al., 2018)*.

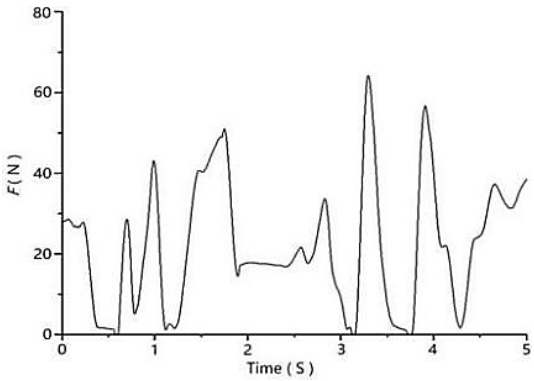

Fig. 8 - The value of the first metatarsal bone in RD gait patterns (after the filtering)

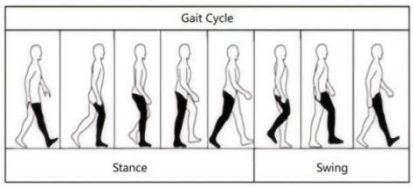

Fig. 9 - Gait cycle

If a gait cycle is effectively segmented, the effective and invalid data can be greatly reduced, and the real-time performance and accuracy of recognition can be obtained. In this paper, the plantar pressure and threshold are used to segment gait phase effectively. The threshold is finally determined as 1/3 of the pressure sum when the user stands still.

Based on previous research on gait, in this paper, two gait events are defined to divide the gait phase. The two gait events are Foot Contact (FC) and Foot Off (FO). FC is the gait event when the pressure rises below a defined threshold reaches the threshold; FO is a gait event when the pressure above the defined threshold drops to a threshold.

Take Fig. 10 as an example to explain a gait cycle. The black curve represents the sum of the three plantar pressure signals, dark blue represents Sensor 1, red represents Sensor 2, and light blue represents Sensor 3. When humans walk on flat ground, they start with the heel off the ground and move forward until the tip of the foot is off the ground. Through the proposed gait segmentation method, a complete gait cycle is divided into four stages by FC and FO: two-station 1 (DS1) and single-station 1 (SS1), two-station 2 (DS2) and single-station 2 (SS2). DS1 is the process of the left foot touching the ground to the right foot leaving the ground, DS2 is the opposite of DS1. SS1 is defined as when the sole of the left foot leaves the ground to when the sole of the left foot touches the ground. Again, SS2 is the opposite of SS1.

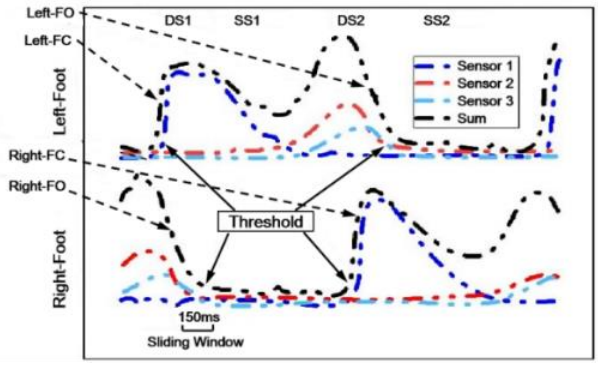

Fig. 10 - Gait segmentation in a gait cycle

Eigenvalue extraction and classifier

Signal eigenvalues are important parameters in locomotion mode recognition and are typically analyzed using window-based analysis and incremental steps. The detailed process is illustrated in Figure 11. During locomotion mode recognition, the eigenvalue of the signal is calculated within each analysis window of duration R. The window then shifts backward by a time interval t, and the eigenvalue for the next analysis window is computed.

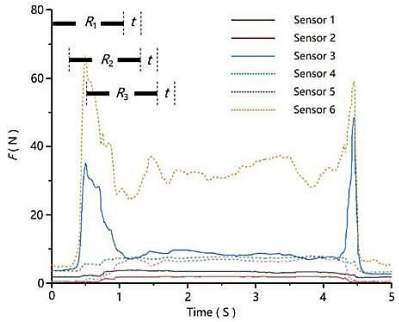

Fig. 11 - The process of eigenvalue extraction

In theory, the duration of the analysis window affects the length of recognition time and whether the current gait pattern is accurately reflected. The increment of the window will also affect the computation amount and recognition delay. The eigenvalue extraction of the signal is related to the sensor signals.

In this paper, a 150 ms sliding window is used to extract the eigenvalue of a total of 14 channels of sensing data (including two IMU sensing signals, each IMU has 4 channels) and pressure data (6 channels).

The sensor type in this paper is a mechanical sensor, the time-domain analysis method is used to extract signal eigenvalues. This method does not need signal transformation, and the calculation is easy and time-consuming. It mainly includes: maximum value, minimum value, mean value, standard deviation, and waveform length (the sum of absolute values of signal changes every 10 ms), where:

Waveform length (WL) is calculated by Equation 9.

$$l_0 = \sum_{k=1}^{N} |\Delta x_k| \tag{9}$$

Standard deviation (STD) is calculated by Equation 10.

$$STD = \sigma = \sqrt{\frac{1}{N-1}\sum_{k=1}^{N}(x_i - \overline{x})^2} \tag{10}$$

In summary, this paper constructs a sliding window of 15×14 matrix through Matlab and extracts the maximum value, minimum value, mean value, standard deviation and waveform length of each signal channel under this sliding window. LDA is a linear discriminant analyzer, which requires relatively low computational complexity and can better reflect the differences between samples by using prior knowledge of categories. Therefore, LDA is selected as the classification method.

The performance of LDA is the important target, its model is constructed and explained. In general pattern recognition, the goal of classification is to pursue the minimum error rate. By using the Bayes rule, the classification decision can be made to minimize errors. When the probability density in Bayes rule is a normal distribution condition, the expression of statistical decision-making is given in Equation 11.

$$P(x|c_i) = \frac{1}{(2\pi)^{d/2}|\Sigma_i|^{1/2}} \times e\left\{-\frac{1}{2}(x-\mu_i)\Sigma_i{}^{-1}(x-\mu_i)^T\right\} \tag{11}$$

where $x = [x_1, x_2, \ldots, x_d]$, x_i is the eigenvalue of the input, x is the corresponding feature vector, that is, the new sample formed after extracting the feature value from the original data. In this paper, the dimension of the feature vector is 1×30, that is, d=30. $\mu = [\mu_1, \mu_2, \ldots, \mu_d]$, μ is the mean of the sample of eigenvalues, Σ_i is the covariance matrix of each class (symmetric nonnegative definite matrix).

For binary problems, it is only necessary to compare the numerator parts of the above formulas. If the two types of samples are separated, a decision surface exists, and the equation of the decision surface can be expressed as shown in Equation 12.

$$g(x) = ln\,P\,(C_i|x) - ln\,P\,(C_j|x)$$
$$g(x) = -\frac{1}{2}\left[(x-\mu_i)\Sigma_i{}^{-1}(x-\mu_i)^T - (x-\mu_j)\Sigma_j{}^{-1}(x-\mu_j)^T\right] - \frac{1}{2}ln\frac{|\Sigma_i|}{|\Sigma_j|} + ln\frac{P(C_i)}{P(C_j)} \tag{12}$$

Assuming that the covariance matrices of each class are equal, i.e., Σ_i=Σ_j=Σ, the decision surface equation $g(x)$ can finally be expressed as shown in Equation 13.

$$g(x) = \omega x^T + \omega_0$$
$$\omega = \ （\mu_i + \mu_j)\Sigma^{-1}$$
$$\omega_0 = -\frac{1}{2}\ （\mu_i + \mu_j)\Sigma^{-1}(\mu_i - \mu_j)^T + ln\frac{P(C_i)}{P(C_j)} \tag{13}$$

where ω and ω_0 are the model parameters. After obtaining the training model, they are directly used in the subsequent online identification test, and the model parameters do not change in the test.

Evaluation method

In our study, K-fold Cross Validation (K-CV) method is used to evaluate the recognition accuracy. In the K-CV method, 10-fold Cross Validation is used. The data of each gait pattern at each gait phase are divided into 10 parts, among which 9 parts are used for classifier training and the remaining one part is used for test data. This process is repeated 10 times to make the 10 parts used as one test data respectively.

Recognition Accuracy (RA) is defined by Equation 14.

$$RA = \frac{Ncor}{Ntotal} \times 100\% \tag{14}$$

where N_{cor} represents the number of correctly identified data groups, and N_{total} indicates the total number of test data groups.

To describe the recognition effect in more detail, a confusion matrix was used, as shown in Eq.15.

$$C = \begin{bmatrix} r_{11} & r_{12} & \cdots & r_{1n} \\ r_{21} & r_{22} & \cdots & r_{2n} \\ \cdots & \cdots & \cdots & \cdots \\ r_{n1} & r_{n2} & \cdots & r_{nn} \end{bmatrix} \tag{15}$$

where each element is described as shown in Equation 16.

$$r_{ij} = \frac{n_{ij}}{n_i} \times 100\% \tag{16}$$

where n_{ij} is the number of gait patterns i recognized as j in the test. n_i denotes the number of gait patterns i in the test. r_{ij} represents the probability that gait pattern i is recognized as j. When i=j, r_{ij} represents the recognition accuracy of gait pattern i.

RESULTS AND DISCUSSIONS

Independent gait pattern recognition performance

The average recognition accuracy of the independent gait pattern is 90.91%, and the recognition accuracy of DS1, DS2, SS1 and SS2 are 90.53%, 91.18%, 90.59% and 91.36%, respectively. The independent gait pattern has 11 gaits pattern in total and contains gaits pattern with similar motion characteristics. Overall, the experimental results are satisfactory. It should be noted here that the SI and ST do not have gait phase, but they are lumped together for the brevity of the confusion matrix. The detailed results are shown in Fig. 12.

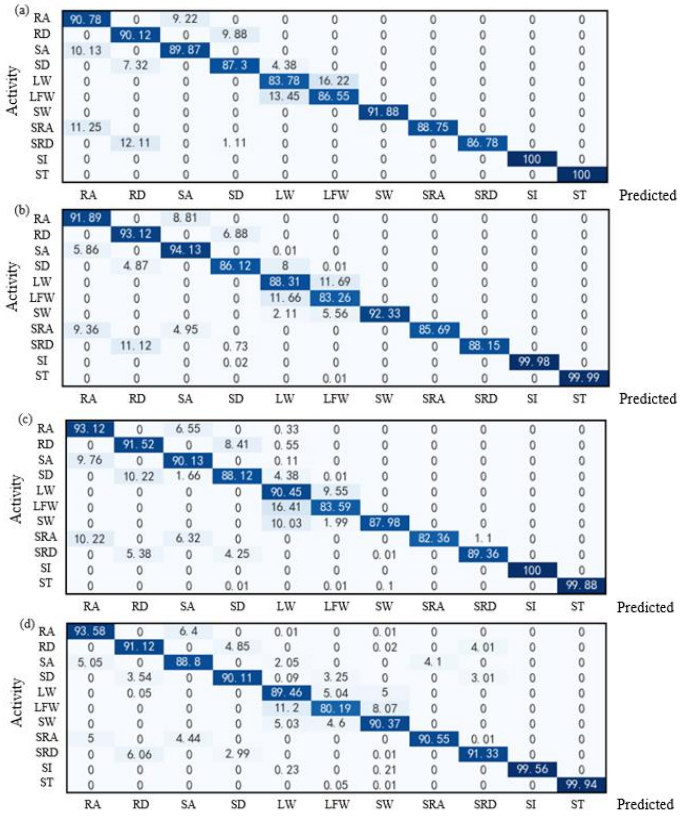

Fig. 12 - The detailed results of the independent gait pattern

(a) DS1 phase; (b) DS2 phase; (c) SS1 phase; (d) SS2 phase

In the above results, the lowest recognition accuracy of the independent gait pattern is 80.19%, which is LFW in SS2 phase. Three flat walking modes are tested: LW, LFW, and SW. By comparing the curves of the plantar pressure system of the three gait patterns (Fig. 13), it can be seen that they have similar motion characteristics, which leads to the identification error. Although the recognition accuracy of LFW in SS2 phase is about 10% different from the average recognition accuracy, the accuracy of 80.19% is acceptable.

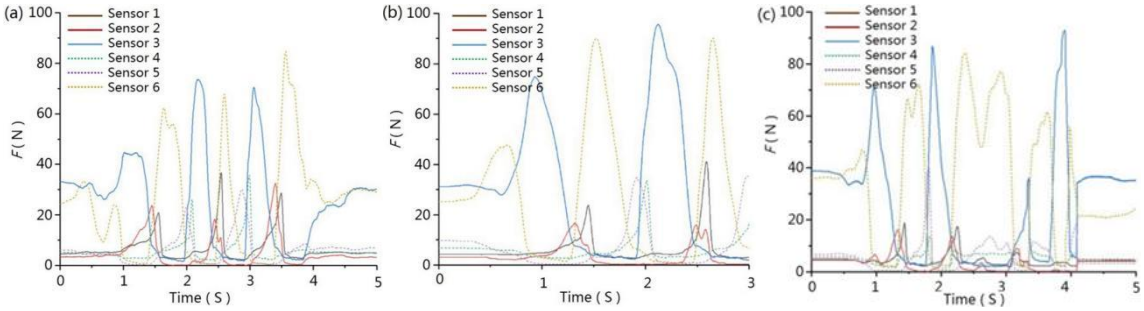

Fig. 13 - The curves of the plantar pressure system of the LW, LFW and SW

(a) LW; (b) LFW; (c) SW

Transformed gait patterns recognition performance

The results of the transformed gait pattern are similar to the independent gait pattern (Fig. 14). Its average recognition accuracy is 92.67%, and the recognition accuracy of DS1, DS2, SS1 and SS2 are 91.93% , 92.79%, 93.31% and 92.65%, respectively.

The lowest recognition accuracy is 85.47%, which is LW-SD in DS1 phase. In DS1, the two highest false recognition rates are LW-SA and SW-SRA, which are 7.20% and 4.02%, respectively. The three gaits pattern have similar motion characteristics. The higher false recognition rate is also due to these similar motion characteristics.

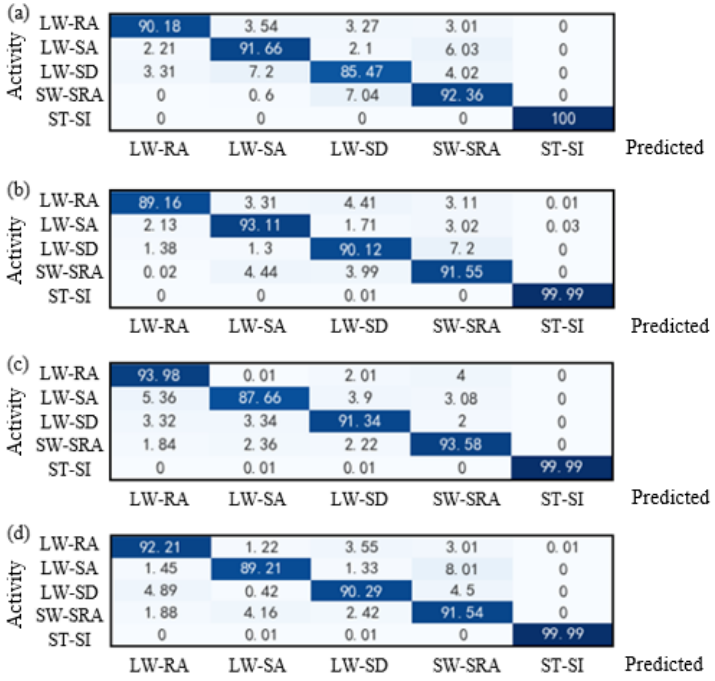

Fig. 14 - The detailed results of transformed gait pattern

(a) DS1 phase; (b) DS2 phase; (c) SS1 phase; (d) SS2 phase

Discussion

Independent gait has been studied relatively early, and the common human locomotion modes are: level walking, ramp ascent, ramp descent, stair ascent and stair descent. At present, the recognition rate of independent gait can reach above 95%. Compared with independent gait, the research time of transformed gait is relatively late, and the recognition is more difficult. At present, most types of gait recognition are less, about 5 – 8, and the road is mostly standardized (Table 2) *(Gao et al., 2020; Liu et al., 2020; Young et al., 2013)*. Because the increase in the number of patterns will affect the recognition accuracy.

Table 2

Comparison of gait

Reference	Independent gait		Transformed gait	
	Number	Accuracy	Number	Accuracy
Gao et al. (2020)	5	98.46%	—	
Liu et al. (2020)	5	95.8%	—	
Young et al. (2013)	5	84.5%	8	93.9%
Our Method	11	90.91%	5	92.67%

In this paper, the number of locomotion modes has been increased. 11 independent gaits and 5 transformed gaits are studied. In addition, the road conditions are much closer to reality. The walking condition in the soil is added, which is more significant in application. The overall accuracy of pattern recognition for both independent and transformed gait is above 90%. This is a relatively satisfactory result.

At present, the main locomotion modes with similar motion curves have affected the accuracy. This may be related to the number of sensor and data processing. The increase in the number of sensor helps with pattern recognition, but it puts an extra burden on amputees' bodies and affects their movement. On the premise of ensuring the recognition accuracy, the use of sensors should be reduced. The recognition rate of the measurement system proposed in this work is above 90%, which achieves the expected goal.

CONCLUSIONS

In this paper, a human lower limb motion data measurement system, which has good environmental adaptability, was presented. Based on data filtering and gait segmentation, LDA classifier is used to analyze the data, and K-CV method is used to judge the accuracy of the results.

The average recognition accuracy of the independent gait pattern is 90.91%, and the highest accuracy of SS2 pattern is 91.36% among the four gait phases. The average recognition accuracy of the transformed gait pattern is 92.67%, and the highest accuracy among the four gait phases is 93.31% of SS1.

This method can accurately predict the locomotion mode of human lower limbs. Intelligent prostheses help lower limb amputees move by controlling joints, they can perform various activities more easily. Since the dynamics and kinematics required by the prosthesis are different in different locomotion modes, it is of great significance to accurately identify the user's locomotion mode for the operation of the prosthesis. Therefore, the method in this paper can provide a reference for the gait recognition, prediction and control strategy of intelligent prostheses.

ACKNOWLEDGEMENTS

This study was supported by the Basic scientific research project of Liaoning Provincial Department of Education (No. JYTMS20231271), China.

REFERENCES

[1] Au, S. K., Weber, J., Herr, H., (2009), Powered ankle-foot prosthesis improves walking metabolic economy. *IEEE Transactions on robotics*, Vol. 25, pp. 51-66. https://doi.org/10.1109/TRO.2008.2008747

[2] Adapala, R. K., Thoppil, R. J., Luther, D. J., Paruchuri, S., Meszaros, J. G., Chilian, W. M., Thodeti, C. K., (2013), TRPV4 channels mediate cardiac fibroblast differentiation by integrating mechanical and soluble signals. *Journal of molecular and cellular cardiology*, Vol. 54, pp. 45-52. https://doi.org/10.1016/j.yjmcc.2012.10.016

[3] Ambrozic, L., Gorsic, M., Geeroms, J., Flynn, L., Lova, R. M., Kamnik, R., Munih, M., Vitiello, N., (2014), CYBERLEGs: A user-oriented robotic transfemoral prosthesis with whole-body awareness control. *IEEE Robotics & Automation Magazine*, Vol. 21, pp. 82-93. https://doi.org/10.1109/MRA.2014.2360278

[4] Anwary, A. R., Yu, H. N., Vassallo, M., (2018), Optimal foot location for placing wearable IMU sensors and automatic feature extraction for gait analysis. *IEEE Sensors Journal*, Vol. 18, pp. 2555-2567. https://doi.org/10.1109/JSEN.2017.2786587

[5] Bisio, I., Delfino, A., Lavagetto, F., Sciarrone, A., (2016), Enabling IoT for in-home rehabilitation: Accelerometer signals classification methods for activity and movement recognition. *IEEE Internet of Things Journal*, Vol. 4, pp. 135-146. https://doi.org/10.1109/JIOT.2016.2628938

[6] Bakina, O. V., Fomenko, A. N., Korovin, M. S., Glazkova, E. A., Svarovskaya, N. V., (2018), An ICA-EBM-based sEMG classifier for recognizing lower limb movements in individuals with and without knee

pathology. *IEEE Transactions on Neural Systems and Rehabilitation Engineering*. Vol. 26, pp. 675-686. https://doi.org/10.1109/TNSRE.2018.2796070

[7] Chen, B. J., Wang, X. G, Huang, Y., Wei, K. L., Wang, Q. N., (2015), A foot-wearable interface for locomotion mode recognition based on discrete contact force distribution. *Mechatronics*, Vol. 32, pp. 12-21. https://doi.org/10.1016/j.mechatronics.2015.09.002

[8] Dey, s., Yoshida, T., Schilling, A. F., (2020), Feasibility of training a random forest model with incomplete user-specific data for devising a control strategy for active biomimetic ankle. *Frontiers in Bioengineering and Biotechnology*, Vol. 8, pp. 855. https://doi.org/10.3389/fbioe.2020.00855

[9] Fan, J. H., Jiang, X. Y., Liu, X. Y., Meng, L., Jia, F. M., Dai, C. Y., (2024), Surface EMG feature disentanglement for robust pattern recognition. *Expert Systems with Applications*, Vol. 237, pp.121224. https://doi.org/10.1016/j.eswa.2023.121224

[10] Gorsic, M., Kamnik, R., Ambrozic, L., Vitiello, N., Lefeber, D., Pasquini, G., Munih, M., (2014), Online phase detection using wearable sensors for walking with a robotic prosthesis. *Sensors*, Vol. 14, pp. 2776-2794. https://doi.org/10.3390/s140202776

[11] Gao, F., Liu, G. Y., Liang, F. Y., Liao, W. H., (2020), IMU-based locomotion mode identification for transtibial prostheses, orthoses, and exoskeletons. *IEEE Transactions on Neural Systems and Rehabilitation Engineering*, Vol. 28, pp. 1334-1343. https://doi.org/10.1109/TNSRE.2020.2987155

[12] Huang, H., Zhang, F., Hargrove, L. J., Dou, Z., Rogers, D. R., Englehart, K. B., (2011), Continuous locomotion-mode identification for prosthetic legs based on neuromuscular–mechanical fusion. *IEEE Transactions on Biomedical Engineering*, Vol. 58, pp. 2867-2875. https://doi.org/10.1109/TBME.2011.2161671

[13] Haladjian, J., Scheuermann, C., Bredies, K., Bruegge, B., (2017), A smart textile sleeve for rehabilitation of knee injuries. *The 2017 ACM International Joint Conference on Pervasive and Ubiquitous Computing and the 2017 ACM International Symposium on Wearable Computers*, pp. 49-52. https://doi.org/10.1145/3123024.3123151

[14] Haladjian, J., Bredies, K., Brugge, B., (2018), KneeHapp textile: A smart textile system for rehabilitation of knee injuries. *IEEE 15th International Conference on Wearable and Implantable Body Sensor Networks (BSN)*, pp. 9-12. https://doi.org/10.1109/BSN.2018.8329646

[15] Hussain, T., Maqbool, H. F., Iqbal, N., Khan, M., Salman, Dehghani-Sanij, A. A., (2019), Computational model for the recognition of lower limb movement using wearable gyroscope sensor. *International Journal of Sensor Networks*, Vol. 30, pp. 35-45. https://doi.org/10.1504/IJSNET.2019.10020697

[16] Hartmann, Y., Liu, H., Schultz, T., (2020), Feature Space Reduction for Multimodal Human Activity Recognition. *Proc of the 13th International Joint Conference on Biomedical Engineering Systems and Technologies*, pp. 135-140. https://doi.org/10.5220/0008851401350140

[17] Hartmann, Y., Liu, H., Schultz, T., (2021), Feature Space Reduction for Human Activity Recognition based on Multi-channel Biosignals. *Proc of the 14th International Conference on Bio-inspired Systems and Signal Processing*, pp. 215-222. https://doi.org/10.5220/0010260802150222

[18] Hartmann, Y., Liu, H., Schultz, T., (2022), Interactive and Interpretable Online Human Activity Recognition. *2022 IEEE International Conference on Pervasive Computing and Communications Workshops and other Affiliated Events (PerCom Workshops)*, pp. 109-111. https://doi.org/10.1109/PerComWorkshops53856.2022.9767207

[19] Hartmann, Y., Liu, H., Lahrberg, S., Schultz, T., (2022), Interpretable High-level Features for Human Activity Recognition. *Proc of the 15th International Joint Conference on Biomedical Engineering Systems and Technologies (BIOSTEC 2022)*, pp. 40-49. https://doi.org/10.5220/0010840500003123

[20] Hernandez, I., Yu, W., (2022), Recent advances on control of active lower limb prostheses. *IETE technical review*, Vol.39, pp. 1225-1244. https://doi.org/10.1080/02564602.2021.1994477

[21] Hartmann, Y., Liu, H., Schultz, T., (2023), Interpretable High-Level Features for Human Activity Recognition and Modeling. *Biomedical Engineering Systems and Technologies*, Vol. 1814, pp.141-163. https://doi.org/10.5220/0010840500003123

[22] Jain, S., Singhal, G., Smith, R. J., Kaliki, R., Thakor, N., (2012), Improving long term myoelectric decoding, using an adaptive classifier with label correction. *In 2012 4th IEEE RAS & EMBS International Conference on Biomedical Robotics and Biomechatronics*, pp. 532-537. https://doi.org/10.1109/BioRob.2012.6290901

[23] Khaleghi, B., Khamis, A., Karray, F. O., Razavi, S. N., (2013), Multisensor data fusion: A review of the state-of-the-art. *Information fusion*, Vol. 14, pp. 28-44. https://doi.org/10.1016/j.inffus.2012.10.004

[24] Liu, M., Zhang, F., Huang, H., (2017), An adaptive classification strategy for reliable locomotion mode recognition. *Sensors*, Vol. 17, pp. 2020. https://doi.org/10.3390/s17092020

[25] Liu, Z. J., Lin, W., Geng, Y. L., Yang, P., (2017), Intent pattern recognition of lower-limb motion based on mechanical sensors. *IEEE/CAA Journal of Automatica Sinica*, Vol. 4, pp. 651-660. https://doi.org/10.1109/JAS.2017.7510619

[26] Liu, H., Hartmann, Y., Schultz, T., (2021), CSL-SHARE: A Multimodal Wearable Sensor-Based Human Activity Dataset. *Frontiers in Computer Science*, Vol. 3, pp. 759136. https://doi.org/10.5220/0010896400003123

[27] Luo, S. L., Shu, X. L., Zhu, H. X., Yu, H. L., (2023), Early prediction of lower limb prostheses locomotion mode transition based on terrain recognition. *IEEE Sensors Journal*, Vol. 23, pp. 27941-27948. https://doi.org/10.1109/JSEN.2023.3320274

[28] Meng, L., Pang, J., Wang, Z. Y., Xu, R., Ming, D., (2021), The role of surface electromyography in data fusion with inertial sensors to enhance locomotion recognition and prediction. *Sensors*, Vol. 21, pp. 6291. https://doi.org/10.3390/s21186291

[29] Nazarpour, K., Sharafat, A. R., Firoozabadi, S. M. P., (2007), Application of higher order statistics to surface electromyogram signal classification. *IEEE Transactions on Biomedical Engineering*, Vol. 54, pp. 1762-1769. https://doi.org/10.1109/TBME.2007.894829

[30] Parri, A., Yuan, K. B., Marconi, D., Yan, T. F., Crea, S., Munih, M., Lova, R. M., Vitiello, N., Wang, Q. N., (2017), Real-time hybrid locomotion mode recognition for lower limb wearable robots. *IEEE/ASME Transactions on Mechatronics*, Vol. 22, pp. 2480-2491. https://doi.org/10.1109/TMECH.2017.2755048

[31] Quintero, D., Villarreal, D. J., Gregg, R. D., (2016), Preliminary experiments with a unified controller for a powered knee-ankle prosthetic leg across walking speeds. *2016 IEEE/RSJ International Conference on Intelligent Robots and Systems (IROS)*, pp. 5427-5433. https://doi.org/10.1109/IROS.2016.7759798

[32] Sensinger, J. W., Lock, B. A., Kuiken, T. A., (2009), Adaptive pattern recognition of myoelectric signals: exploration of conceptual framework and practical algorithms. *IEEE Transactions on Neural Systems and Rehabilitation Engineering*, Vol. 17, pp. 270-278. https://doi.org/10.1109/TNSRE.2009.2023282

[33] Silva Júnior, W. C., Oliveira, M. A. V. D., Bonvent, J. J., (2015), Conception, design and development of a low-cost intelligent prosthesis for one-sided transfemoral amputees. *Research on Biomedical Engineering*, Vol. 31, pp. 62-69. https://doi.org/10.1590/2446-4740.0647

[34] Tucker, M. R., Olivier, J., Pagel, A., Bleuler, H., Bouri, M., Lambercy, O., Millán, J. D. R., Riener, R., Vallery, H., Gassert, R., (2015), Control strategies for active lower extremity prosthetics and orthotics: a review. *Journal of NeuroEngineering and Rehabilitation*. Vol. 12, pp. 1-30. https://doi.org/10.1186/1743-0003-12-1

[35] Tharwat, A., Gaber, T., Ibrahim, A., Hassanien, A. E., (2017), Linear discriminant analysis: A detailed tutorial. *AI communications*, Vol. 30, pp. 169-190. https://doi.org/10.3233/AIC-170729

[36] Varol, H. A., Sup, F., Goldfarb, M., (2010), Multiclass real-time intent recognition of a powered lower limb prosthesis. *IEEE Transaction on Biomedical Engineering*, Vol. 57, pp. 542-551. https://doi.org/10.1109/TBME.2009.2034734

[37] Wang, K. J., Hou, B. B., (2007), A survey of gait recognition. *Journal of Image and Graphics*, Vol. 12, pp. 1152-1160. https://doi.org/10.3969/j.issn.1006-8961.2007.07.002

[38] Wang, X. G., Wang, Q. N., Zheng, E. H., Wei, K. L., Wang, L., (2012), A wearable plantar pressure measurement system: design specifications and first experiments with an amputee. *Intelligent Autonomous Systems 12: Volume 2 Proceedings of the 12th International Conference IAS-12(Jeju Island, Korea. Springer Berlin Heidelberg)*, pp. 273-281. https://doi.org/10.1007/978-3-642-33932-5_26

[39] Windrich, M., Grimmer, M., Christ, O., Rinderknecht, S., Beckerle, P., (2016), Active lower limb prosthetics: a systematic review of design issues and solutions. *Biomedical Engineering Online*, Vol. 15, pp. 5-19. https://doi.org/10.1186/s12938-016-0284-9

[40] Wang, Q. N., Zheng, E. H., Chen, B., J., Mai, J. G., (2016), Recent progress and challenges of robotic lower-limb prostheses for human robot integration. *Acta Automatica Sinica.* Vol. 42, pp. 1780-1793. https://doi.org/10.16383/j.aas.2016.y000007

[41] Young, A. J., Simon, A. M., Hargrove, L. J., (2013), A training method for locomotion mode prediction using powered lower limb prostheses. *IEEE Transactions on Neural Systems and Rehabilitation Engineering*, Vol. 22, pp. 671-677. https://doi.org/10.1109/TNSRE.2013.2285101

[42] Young, A. J., Simon, A. M., Hargrove, L. J., (2013), A training method for locomotion mode prediction using powered lower limb prostheses. *IEEE Transactions on Neural Systems and Rehabilitation*

Engineering, Vol. 22, pp. 671-677. https://doi.org/10.1109/TNSRE.2013.2285101

[43] Young, A. J., Ferris, D. P., (2016), State of the art and future directions for lower limb robotic exoskeletons. *IEEE Transactions on Neural Systems and Rehabilitation Engineering*, Vol. 25, pp. 171-182. https://doi.org/10.1109/TNSRE.2016.2521160

[44] Yang, J. Q., Yang, L., Ma, Y., (2016), Learning vector quantization neural network-based model reference adaptive control method for intelligent lower-limb prosthesis. *Advances in Mechanical Engineering*, Vol. 8, pp. 1-13. https://doi.org/10.1177/1687814016647354

[45] Yuan, K. B., Wang, Q. N., Wang, L., (2017), Energy-efficient braking torque control of robotic transtibial prosthesis. *IEEE/ASME Transactions on Mechatronics*, Vol. 22, pp. 149-160. https://doi.org/10.1109/TMECH.2016.2620166

[46] Yue, L., Lu, Z. X., Hui, D., Chao, J., Liu, Z. Q., Liu, Z. J., (2023), How to Achieve Human-Machine Interaction by Foot Gesture Recognition: A Review. *IEEE Sensors Journal*, Vol. 23, pp. 16515-16528. https://doi.org/10.1109/JSEN.2023.3285214

[47] Zhu, J. Y., Wang, Q. N., Wang, L., (2014), On the design of a powered transtibial prosthesis with stiffness adaptable ankle and toe joints. *IEEE Transactions on Industrial Electronics*, Vol. 61, pp. 4797-4807. https://doi.org/10.1109/TIE.2013.2293691